IMPACT OF THE EXPANSION OF URBAN IMPERVIOUS SURFACES ON CYANOBACTERIAL BLOOM IN THE BILLINGS RESERVOIR, SP - BRAZIL

Thainara Munhoz Alexandre de Lima[1], Rômulo Marques Carvalho[1], Cláudia Maria de Almeida[1], Claudio Clemente Faria Barbosa[1], Thales Sehn Körting [1]

[1]Programa de Pós-Graduação em Sensoriamento Remoto - PGSER, Divisão de Observação da Terra e Geoinformática - DIOTG, Instituto Nacional de Pesquisas Espaciais - INPE

ABSTRACT

This paper aims to apply the digital processing of satellite images to assess the relationship between the expansion of impermeable surfaces and cyanobacterial proliferation. For this purpose, the Billings reservoir, located in the Metropolitan Region of São Paulo, Brazil, was adopted as the object of the study. The urban expansion in the hydrological watershed where this reservoir is located and the increase of cyanobacteria concentration in its water were quantified. The results show that there is a positive linear relationship between the increase in impervious surfaces and the proliferation of cyanobacterial colonies. However, this study did not quantify this relationship, what is intended to be explored in future works.

Index Terms— Remote sensing, impervious surface, cyanobacterial, Billings reservoir, São Paulo.

1. INTRODUCTION

Continental aquatic systems play a relevant role in the full exercise of citizenship and in the sustainable development of a country. As reported by Azevedo *et al*. (2006) [1] and Smith and Schindler (2009) [2], despite the great importance of these systems, anthropic activities such as agriculture, urbanization, and deforestation have promoted the eutrophication of water bodies [3].

With regard to the effects of urbanization, these include changes in the geomorphology and hydrology of aquatic environments in urban areas, decrease in biodiversity, dominance of toxic species, and increase in concentration of organic compounds, nutrients, and biomass of cyanobacteria [4]. The proliferation of cyanobacteria and the consequent eutrophication of a water body can impact both the human population and the local fauna and flora, significantly altering the local ecosystem [5].

This is the case of the springs that integrate the water supply system of the Metropolitan Region of São Paulo (RMSP), whose estimated population of 21,252,384 inhabitants have intensely impacted the springs with domestic and industrial sewage, deforestation, erosion, and irregular land use [6]. In 2020, 12 new groups of bacteria were found in Billings that until then had not been detected, making the reservoir a “black box” of sediments that can cause increasing damage to public health. Thus, the objective of this study is to evaluate the relationship between expansion of urban impervious surfaces in the Billings-Tamanduateí watershed, one of the hydrographic units for management purposes in RMSP, also known as Great São Paulo, and the seasonal variation of cyanobacterial blooms in the Billings reservoir, between the 1990s and 2020.

2. MATERIAL AND METHODS

2.1. Remote sensing data and impervious surface estimation

The proposed methodology uses Landsat Collection 2 Level-2. Due to the analysis time interval, it was necessary to use images from two sensors: Landsat-5/TM and Landsat-8/OLI surface reflectance (SR) products. The surface reflectance images were cropped with a Shapefile of the Billings-Tamanduateí watershed perimeter. Then, the classification was performed from the B5 (Short-wave Infrared), B4 (Near Infrared) and B3 (red) bands of the TM sensor and the B6 (Short-wave Infrared SWIR 1), B5 (Near Infrared) and B4 (red) bands of the OLI sensor. For the sampling process, two categories were adopted: permeable covers (water, soil, and vegetation) and impermeable covers (urbanized surfaces). Finally, an independent pixel-based classification was performed with the Random Forest algorithm to each year. From the totality of the samples, 70% were meant for algorithm training and 30% for validation. For quality assessment, the accuracy and the F1-Score were calculated. All digital image processing was implemented in QGIS 3.16.3 software.

2.2. Remote sensing of Chl-a concentration

2.2.1. Landsat imagery pre-processing

The Landsat-5/TM product was generated by applying the LEDAPS (Landsat Ecosystem Disturbance Adaptive Processing System) algorithm for atmospheric correction [7], and Landsat-8 SR data was obtained from LaSRC (Land Surface Reflectance Code) algorithm [8]. The sun glint effect was corrected by subtracting the B6 (1.61 µm) for OLI images and B5 (1.65 µm) from TM images. To reduce adjacency effects, the NDWI (Normalized Difference Water Index) was applied, which is one of the most commonly used water indices to delineate features present in

the aquatic environment and highlight their presence in the images.

2.2.2. Field radiometric data

We accessed in situ radiometric data from the Instrumentation Laboratory for Aquatic System (LabISA) (http://www.dpi.inpe.br/labisa/) database in the Brazilian National Institute for Space Research (INPE), collected in the Billings Reservoir and from CETESB (São Paulo State Environmental Company). Resulting in a total of 32 samples. Details about the field campaigns can be found in Lobo et al. (2021) [9]. Due to the limited numbers of Chl-a in situ samples available on the same day as the satellite image acquisition, a time window of 2 days was considered to gather a larger number of samples.

2.2.3. Calibration and validation of semi-empirical model

The estimation of the Chl-a concentration was made using the Normalized Difference Chlorophyll Index (NDCI) developed by Mishra and Mishra (2012) [10]. Studies have demonstrated the high accuracy of NDCI in different aquatic environments with varying concentrations of Chl-a. In Landsat-5/TM model, B3 (0.66 µm) and B4 (0.83 µm) were used, whilst in Landsat-8/OLI bands B4 (0.655 µm) and B5 (0.865 µm) were used. In order to normalize the radiometric differences between the TM and OLI, a model based on the in situ radiometric data was developed, where the calculated NDCI for the OLI was normalized with the NDCI for TM. The purpose of this normalization was the calibration of a single empirical model for estimating Chl-a that can be used in both sensors.

For the calibration of the empirical model used for Chl-a estimation, the bands of Landsat-5/TM were simulated from in situ R_{rs}, as well as the spectral response function available on the United State Geological Survey website (https://landsat.usgs.gov/spectral-characteristics-viewer). Based on the TM simulated bands, the NDCI was calculated and a relationship was established between the measured in situ Chl-a concentrations and the NDCI values. The model was calibrated testing linear and polynomial (second degree) adjustments. A 26-sample dataset corresponding to all the match-ups between in situ Chl-a data and NDCI from satellite image were used to calibrate the Chl-a algorithm, both for the linear and the polynomial fit. For model validation the statistical metrics used were: Root Mean Square Error (RMSE); Mean Absolute Percentage Error (MAPE); and Coefficient of Determination (R2).

3. RESULTS

3.1. Impervious surface estimation

The total area of the Billings-Tamanduateí watershed is 824.05 km², with predominantly pervious surfaces. In 1991, the percentage of impervious surface already reached 25%, i.e., about 204.88 km². In 2001, this area increased to 275.26%, accounting for 33% of imperviousness in the watershed. From then on, the cumulative expansion of impervious surface increased by 1% for each 10 years, which represented an area of 278.51 km² and 286.90 km² in 2011 and 2020, respectively. The spatialization of these results is presented in Fig.1.

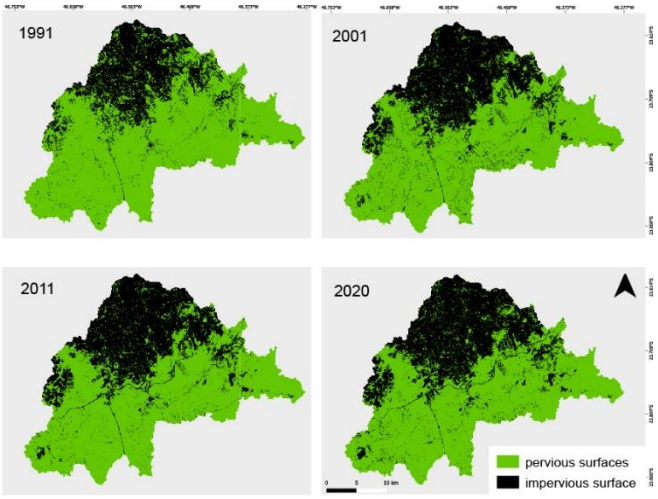

Figure 1 – Expansion of urban impervious surfaces in the Billings-Tamanduateí watershed. The panels present each considered year: 1991, 2001, 2011 and 2020.

The 1991 map has an overall accuracy of 97% and F1-Score equal to 0.97. The 2001 map, on the other hand, achieved a lower overall accuracy, around 92%, and F1-Score equal to 0.92. The overall accuracy of the 2011 map was estimated at 94% and F1-Score at 0.94. Finally, the 2021 map has an overall accuracy of 96% and F1-Score of 0.96.

3.2. Chl-a concentration

High values for MAPE (283.15% for linear and 243.99% for pol.) and RMSE (144.35 $mg.m^{-3}$ for linear and 122.46 $mg.m^{-3}$ for pol.) were obtained. Analyzing the residuals of the polynomial model, it can be observed that the algorithm overestimated the Chl-a by an average of 96 mg/m^3. As explained, validation based on CETESB data considered a 2-day match-up interval between the measurement time and the satellite pass. In addition, the model calibration was done using a small number of samples, which may not have been representative of the population. This corroborates the evidence that optical complexity of inland waters, with inputs of solutes and particles from the drainage basin, results in a high temporal and spatial variability of the concentration of Chl-a in the mixture, and that empirical algorithms are limited for application in specific periods and concentrations of Chl-a.

Although both models overestimate the Chl-a concentration, in both, linear and polynomial model, the NDCI presented satisfactory correlation with Chl-a (R=0.883

for linear and R=0.913 for polynomial model), where the best results were obtained with the polynomial model, which also presented a lower overestimation of Chl-a than the linear model. Due to its best results, the polynomial model was applied to NDCI images from Landsat-5/TM and Landsat-8/OLI to retrieve Chl-a concentrations (Fig. 2).

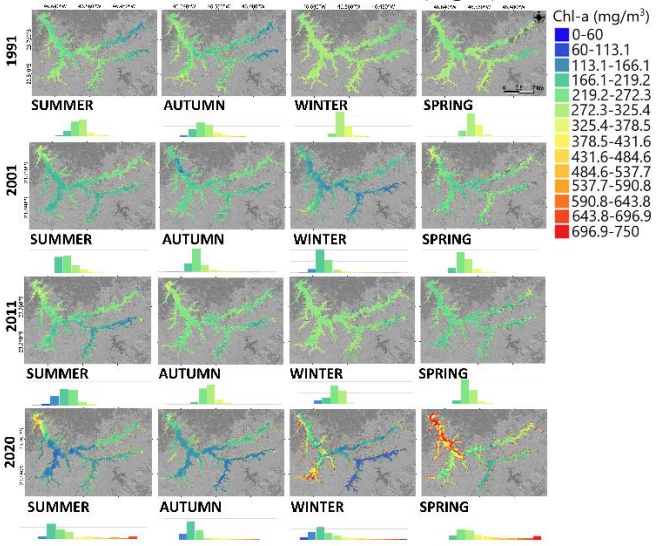

Figure 2 - Seasonal distribution of Chl-a concentration (mg.m-3) in the Billings Reservoir. The panels present each considered year: 1991, 2001, 2011 and 2020. The colored bars represent the histogram for each concentration.

In general, the Chl-a concentration presents spatial variation and seasonal changes across the reservoir: in 1991 high concentration values were observed during winter and spring (Fig.2; Table 1), with much of the reservoir showing a concentration of chl-a above 180 mg.m^{-3} (Table 1) (90.20 km^2 and 74.32 km^2 for winter and spring, respectively). Similar behavior is observed in 2020, with a higher concentration of Chl-a during winter and spring (Fig.2; Table 1). In summer, in general, a lower concentration of Chl-a is observed in all considered years (Fig.2), due to the higher levels of precipitation (Fig.3).

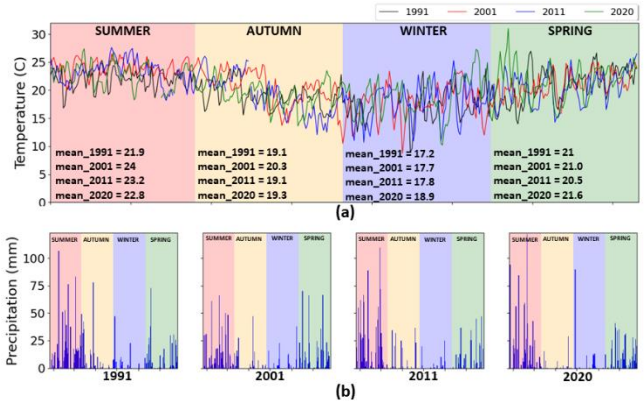

Figure 3 - Time-series of seasonal meteorological parameters in Sao Paulo. (a) Daily average temperature (ºC). (b) Accumulated daily precipitation (mm).

The seasonal behavior of temperature and precipitation in São Paulo favors the high concentration of cyanobacteria in the reservoir in the whole year, the high temperatures in summer and spring and low levels of precipitation during autumn and winter (Fig. 3) significantly reduce the water level and favor the stratification process, reducing vertical mixing, causing cyanobacteria to accumulate in dense superficial blooms [5].

In general, greater bloom intensity is observed in the northern portion of the reservoir that follows the main arm. In the eastern portion, the reservoir has two branches: Rio Grande (northern) and Rio Pequeno (further south) (Fig.2). Due to the high levels of cyanobacteria in the reservoir, in 1982 the Rio Grande was isolated from the Billings system, being currently used for public water supply, and therefore it has a different behavior than the rest of the reservoir (Fig.2), with a lower concentration of Chl-a in general. In the southwestern portion of the reservoir, the arm (Braço, in Portuguese) Taquacetuba is located, which showed high levels of Chl-a concentration in 1991, with a decrease in 2001 and 2011, and again a significant increase during the winter in 2020, as it can be seen in the distribution of pixels (%) in the colored bars (Fig.2).

Chl-a concentrations		>280	>350
Summer	1991	41.14 km²	6.99 km²
	2001	21.24 km²	5.61 km²
	2011	31.12 km²	5.92 km²
	2020	24.84 km²	18.98 km²
Autumn	1991	36.89 km²	11.32 km²
	2001	18.10 km²	4.18 km²
	2011	50.02 km²	7.85 km²
	2020	20.61 km²	14.83 km²
Winter	1991	90.20 km²	10.86 km²
	2001	9.71 km²	3.19 km²
	2011	21.08 km²	2.71 km²
	2020	37.40 km²	27.59 km²
Spring	1991	74.32 km²	10.07 km²
	2001	30.71 km²	5.05 km²
	2011	20.80 km²	3.35 km²
	2020	65.41 km²	45.17 km²

Table 1 - Seasonal variations of the reservoir area with Chl-a concentrations above 280 mg.m^{-3} and 350 mg.m^{-3}. The areas highlighted in orange represent the highest area values over the years, in each season.

4. DISCUSSION

From statistical data extracted through the analysis of the classification presented in Fig. 1, it can be observed that the rate of increase of impervious surface achieved its highest value between 1991 and 2001 (Fig. 4). This process is linked to the installation of large supermarket chains and the intensification of tertiary activities and verticalization in some municipalities in the southern portion of RMSP, the so-called ABC Paulista Region [11]

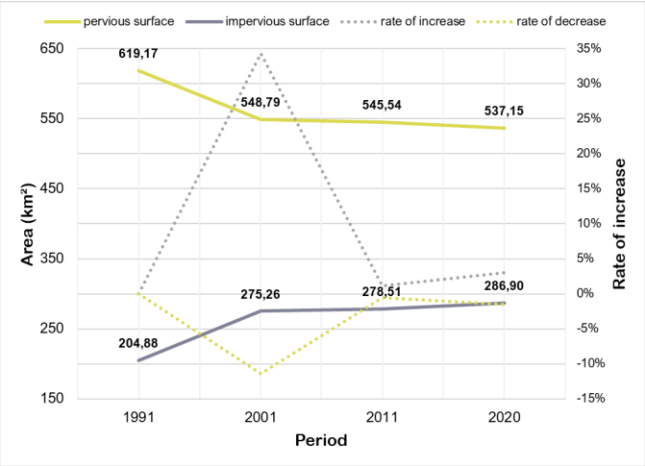

Figure 4 – Statistical data of impervious surface estimation in the Billings-Tamanduateí watershed.

When the impervious surface data were cross-checked with the cyanobacterial coverage data, a positive linear relationship of increase between these variables was observed (Fig. 5). The exception is registered between 1991 and 2001, because in 1989, the continuous reversion of waters from the Tietê River and affluents, through the Pinheiros River, to Billings was prohibited [12], which certainly resulted in a reduction of organic material discharge into the reservoir. In addition, from 1989 onwards, the preservation and recovery of water resources began to be guaranteed by the Constitution of São Paulo, and discussions began on reversing the dam's pollution situation [12].

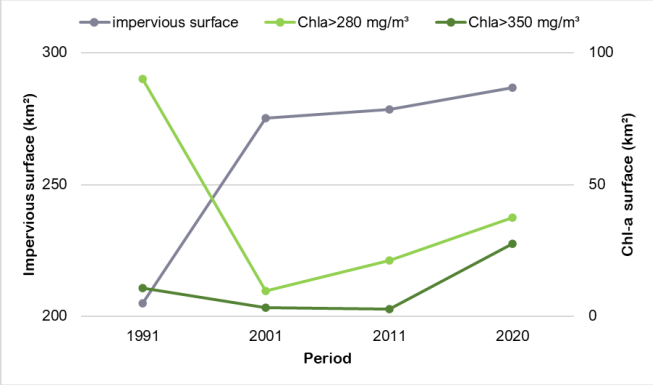

Figure 5 – Relationship between impervious surface and Chla surface.

Despite the decrease observed in 2001, from 2011 onwards, an increase in the concentration of Chl-a is again observed (Fig. 5; Table 1). When observing the areas with concentrations above 350 mg.m^{-3} (Table 1), 2020 presents the largest areas, showing the current critical situation the dam is passing through. The situation observed in 2020, where a high concentration of Chl-a is highlighted in the main arm of the reservoir (Fig.2), shows that the idealized projects tended to fail, and that Billings is currently more polluted than ever.

5. CONCLUSION

The main objective of the present work was to analyze the relationships between the urban expansion process and the variations in the concentration of Chl-a in the Billings Reservoir. The analysis was based on the classification of impermeable areas as well as on the seasonal estimate of Chl-a over a 30-year time series.

The obtained results foster discussions about the consequences of the lack of urban planning and the intense occupation that occurred in the reservoir surroundings. The reported consolidation of the occupations led to the discharge of effluents (domestic, industrial and agricultural) directly into water bodies, an improper disposal of garbage, and the loss of vegetation cover due to indiscriminate deforestation. Over the years, the reservoir portrays the challenges and burdens imposed by the disorderly growth of Sao Paulo city, with a significant increase in the concentration of Chl-a in the water body.

Future studies should focus on using a more robust and representative training dataset to estimate the concentration of Chl-a, thus allowing for the estimation of a more accurate model. Furthermore, despite the results show a positive linear relationship between the increase in impervious surfaces and the proliferation of cyanobacterial colonies, this study did not quantify such relationship, and this is therefore a direction for future research as well.

6. REFERENCES

[1] AZEVEDO, S. M. F. O. VASCONCELOS, V. M. Toxinas de cianobactérias: Causas e Consequências para a saúde pública. Ecotoxicologia Aquática – Princípios e Aplicações. 2006.
[2] SMITH, V.H.; SCHINDLER, D.W. Eutrophication science: where do we go from here? Trends in Ecology Evolution, 24(4), p.201-207, 2009.
[3] RINDI, F. Diversity, distribution and ecology of green algae and cyanobacteria in urban habitats. Algae and cyanobacteria in extreme environments, p. 619-638, 2007.
[4] MEYER, J. L., PAUL, M. J., & TAULBEE, W. K. Stream ecosystem function in urbanizing landscapes published by: the North American Benthological. Society, 24,602–612. 2005.
[5] PAERL, H.W.; HUISMAN, J.Blooms Like it Hot. Science, v. 320, p. 57-58, 2008.
[6] SENDACZ, S. & KUBO, E. Zooplâncton de reservatórios do Alto Tietê, Estado de São Paulo. In Ecologia de reservatórios: estrutura, função e aspectos sociais. São Paulo (R. Henry, ed.). Fapesp, São Paulo, p.509-530. 1999.
[7] CABALLERO, C. E. et al. Assessment of Landsat 5 images atmospherically corrected with LEDAPS in water quality time series. Canadian Journal of Remote Sensing, 2019.
[8] VERMONTE, E. et al. LaSRC: Overview, application and validation using MODIS, VIIRS, Landsat and Sentinel 2 data's. IGARSS, 2018.
[9] LOBO, F. L. et al. AlgaeMAp: Algae Bloom Monitoring Application for Inland Waters in Latin America. Remote Sensing, 2021.
[10] MISHRA, S.; MISHRA, D.R. Normalized difference chlorophyll index: A novel model for remote estimation of chlorophyll-a concentration in turbid productive waters. Remote Sensing of Environment. 117, p. 394-406, 2012.
[11] São Paulo, *Expansão da área urbana da região metropolitana de São Paulo*, Emplasa, São Paulo, 2002.
[12] São Paulo, *Billings*, SMA/CEA, São Paulo, 2010.